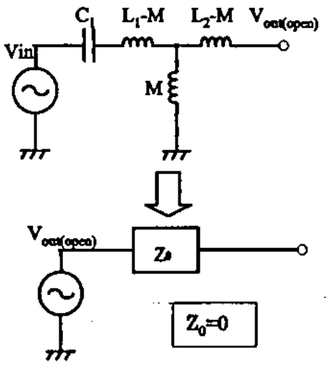

FIG. 2. Helmholtz equivalent circuit.

$$C_1=\frac{1}{{}^2L_1\;1\;\;k^2}.$$

The number N_1 of windings of primary coil is decided from ratio of the voltage

$$\left.\frac{V_{\text{out open}}}{V_{\text{in}}}\right|_{Z_0=0}=\frac{1}{k}\sqrt{\frac{L_2}{L_1}}.$$

In the common contactless power supply systems use detachable transformers. However, our goal is a more flexible power supply system; if the distance between coils or the location of coils changes, the coupling factor k will vary and the minimum internal impedance condition will break. Setting C_2 to an appropriate value can stabilize the output voltage within the range of gap change. (see Fig. 3).

III. SYNCHRONOUS RECTIFICATION

The synchronous rectifier circuit is shown in Fig. 4, where metal-oxide-semiconductor field effect transistor (MOSFETs) synchronize to the diodes. This operation reduces the diodes' voltage drops. Figure 5 shows wave forms of V_1, V_2, and gate voltages of Q_3, Q_4. When V_1 is higher than the threshold voltage Vth of 3.5 V and V_2 is lower than Vth, the gate control circuit turns MOSFETs Q_1 and Q_4 on. In the case where contrary V_2 is higher and V_1 is lower, it turns MOSFETs Q_2 and Q_3 on. Both V_1 and V_2 are lower than Vth, which turns all the MOSFETs off. This operation has a very important role. The switching timings depend on diodes. This prevents the system from malfunctions, such as shoot-through conditions.

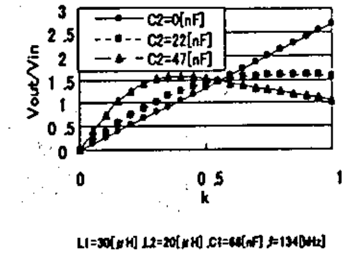

FIG. 3. Output voltage vs coupling factor k: 47 [nF] is the suitable value for C_2.

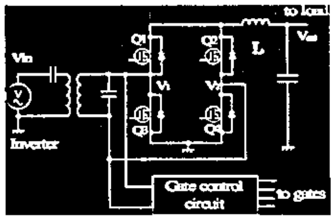

FIG. 4. Synchronous rectifier circuit.

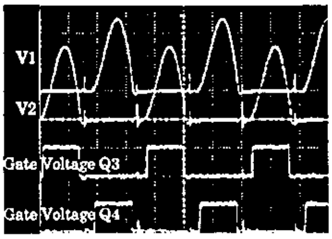

FIG. 5. Wave forms of the synchronous rectifier circuit.

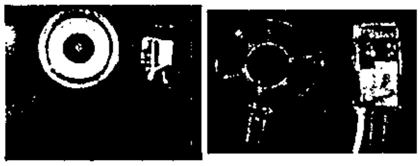

FIG. 6. Contactless power supply system for an artificial heart. Primary unit (left) has a 120-mm-diam coil and a high frequency inverter. Secondary unit (right) has 80-mm-diam coil and a synchronous rectifier unit that is 75 mm high, 40 mm wide and 16 mm thick.

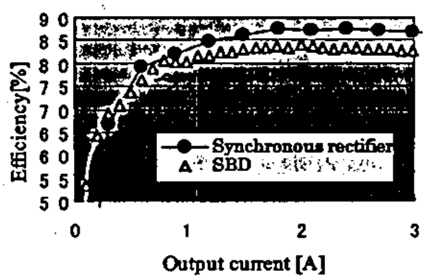

FIG. 7. Efficiency vs output current. Where 88% maximum efficiency (dc to dc) was achieved. The maximum efficiency of the system utilizing schottky barrier diodes is 84%.

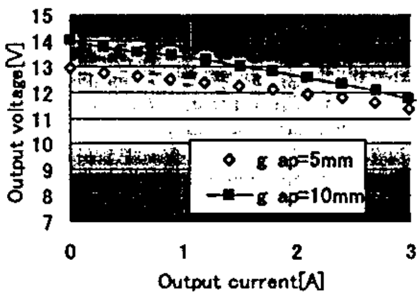

FIG. 8. Output voltage vs output current characteristics was measured at 5 and 10 mm distances between coils.

IV. RESULTS AND DISCUSSION

In Fig. 6, the contactless power supply system we have developed for an artificial heart is shown.[4] This system operates at 190 kHz, and we use planar coils with Mn–Zn ferrite cores. The efficiency of the contactless power supply with synchronous rectifier is 88[%] maximum (dc-dc). Efficiency has been improved by four points compared with the one in which surface behavior diagram were used (Fig. 7). Under 3[A] output current, the output voltage varies 2.6 V . The output voltage is very stable (Fig. 8). We have period in which all the MOSFETs are off. In this period, current runs through the diodes, the loss increase and V_1 and V_2 are low at same time; this means voltage of the secondary coil is distorted. Improvement of the gate control circuit to reduce all MOSFETs off time is necessary. Power consumption of each component should be clarified. We are trying to eliminate the capacitor C_2 and the inductor L, because these are huge components.

V. CONCLUSION

A method for systematic circuit parameter determination was examined. A contactless power supply system with synchronous rectifier was constructed. The system achieved 88% maximum efficiency and highly stable output voltage.

We still have the possibility of improving efficiency, because current runs through diodes in the long periods that all the MOSFETs are turned off. Also, we are making an effort to miniaturize the rectifier unit with the elimination of the huge inductor and resonant capacitor.

[1] J. C. Schuder, H. E. Stephenson, and J. F. Townsend, IRE Int. Conv. Rec. 9, 119 (1961).
[2] H. Matsuki, K. Nadehara, T. Watanabe, K. Murakami, and T. Yamamoto, IEEE Trans. Magn. 25, 3812 (1989).
[3] H. Sakamoto and K. Harada, IEEE Trans. Magn. 29, 3228 (1993).
[4] Y. Abe, T. Chinzei, T. Isoyama, T. Ono, S. Mochizuki, I. Saito, K. Iwasaki, M. Ishimaru, T. Karita, A. Kouno, K. Baba, and K. Imachi, Artif. Organs 25, 69 (2001).

演 題 2

Autonomic Nervous System and Oxygen Metabolism of the Brain during Bathing

Tomoyuki Yambe[1]　Naoki Owada[1]　Yasuyuki Shiraishi[1]　Makoto Yoshizawa[2]
Akira Tanaka[3]　Ken-ichi Abe[3]　Mune-ichi Shibata[1]　Tasuku Yamaguchi[1]
Xudong Duan[1]　Shu Wie[1]　Hiroshi Sasada[4]　Shinichi Nitta[1]

Summary

The dynamic state of circulation during bathing has been studied yet there are very few reports on the dynamic state of blood circulation of blood vessels in the brain. Research on blood flow in the brain has developed through the invention and use of a near-infrared monitoring device (NIRO). We conducted research on heart rate variability (HRV) and oxygen metabolism in brain tissue of the frontal lobe during bathing. We measured the electrocardiogram and blood pressure. The NIRO monitoring device was attached to the subject's frame. The subject then bathed for 20 minutes. Simultaneously with the electrocardiogram, the oxidization hemoglobin concentration of a NIRO monitoring device and TOI were recorded on the data recorder. Quantitative evaluation, statistical handling, and spectrum analysis of data were performed. The data for the 10 minutes before bathing were compared with the data for the 10 minutes after bathing. During measurement, the blood circulation dynamic state was stabilized and the heart rate and blood pressure were maintained within a normal range. The heart rate increased significantly during bathing, while blood pressure decreased significantly. Although HF of heart rate variability increased slightly during bathing, it was not significant. Although LF/HF increased slightly during bathing, it was not significant. Our research found that blood pressure falls during bathing and the heart rate increases. This is considered due to the peripheral blood vessel being opened by bathing. If a peripheral blood vessel opens, blood vessel resistance will fall. To maintain blood pressure, the heart rate goes up. If the heart rate goes up, cardiac output increases. If cardiac output increases, blood pressure returns. Autonomic nerves play an active part in this process. HF and LF/HF increased slightly. This data supports this reaction. O_2Hb and TOI increased slightly during bathing. This result suggests an increase in brain blood flow. Intellectual activity was not carried out during bathing. It is considered that O_2Hb increased because supply increased. The result of TOI also supported this consideration. Intracere-

Running head：Brain Oxygenation during Bathing

Key words：Taking bath, Near infrared spectroscopy, Heart rate variability, Spectral analysis, Stroke

[1] Department of Medical Engineering and Cardiology, Institute of Development, Aging and Cancer, Tohoku University [2] Information Synergy Center, Tohoku University [3] Tohoku University Graduate School of Engineering [4] Tohoku University Graduate School of Agriculture

Address correspondence and reprint request to：Tomoyuki Yambe, M. D., Ph.D., F. J. C. C., F. J. S. I. C., Department of Medical Engineering and Cardiology, Institute of Development, Aging and Cancer, Tohoku University. 4-1 Seiryo-machi, Aoba-ku, Sendai 980-77, Japan. Tel：81-22-717-8514 or 8517, Fax：81-22-717-8518, e-mail：yambe @ idac.tohoku.ac.jp

bral bleeding during bathing may originate in the increase in blood flow. The fall of blood pressure may be desirable. If blood pressure falls, brain blood flow will fall in those who have arteriosclerosis in a brain artery. The fall of a brain blood flow relates to cerebral infarction. Sick people need to be cautious when bathing.

Introduction

Bathing is a traditional Japanese custom. From ancient times, Japanese people have maintained the cleanliness of the body by bathing. In fact, bathing is considered central in Japan for public health. There are the various features of bathing in Japan. Japanese bathe in hotter water than in western countries. Though regrettable, there are many accidents caused by bathing in Japan. For example, many elderly people exhibit symptoms of heart attack or apoplexy during bathing.

The dynamic state of circulation during bathing has been studied yet there are very few reports on the dynamic state of blood circulation of blood vessels in the brain[1-9]. Research on blood flow in the brain has developed through the invention and use of a near-infrared monitoring device (NIRO). There are many research reports on anesthesia and operations using NIRO, but there is little research that considers lifestyle. We conducted research on heart rate variability (HRV) and oxygen metabolism in brain tissue of the frontal lobe during bathing[10-14]. Since interesting results were observed, we have analyzed the results and present our findings here.

Material and method

Study subjects were 10 healthy men. We measured the electrocardiogram and blood pressure. The NIRO monitoring device was attached to the subject's frame. At bed rest, the measurement was performed for 10 minutes. The subject then bathed for 20 minutes. Simultaneously with the electrocardiogram, the oxidization hemoglobin concentration of a NIRO monitoring device and TOI were recorded on the data recorder. Quantitative evaluation, statistical handling, and spectrum analysis of data were performed. The data for the 10 minutes before bathing were compared with the data for the 10 minutes after bathing.

Results

Measurement stabilization was possible in the 10 subjects. During measurement, the blood circulation dynamic state was stabilized and the heart rate and blood pressure were maintained within a normal range.

Fig. 1 shows the rise of the temperature under bathing. By a diagram, it turns out during bathing that temperature is rising. The heart rate under bathing and change of blood pressure are illustrated in the **Fig. 2,3.** The heart rate increased significantly during bathing, while blood pressure decreased significantly. The brain tissue oxygen metabolism of the frontal lobe is shown to **Fig. 4.** Although O_2Hb was not significant, it showed an upward trend. The tissue oxygen index (TOI) in the brain tissue of the frontal lobe is shown to **Fig. 5.** Although TOI was not so significant altered. The spectrum analysis result of a heart rate variability is shown to **Fig. 6,7.** Although HF of heart rate variability increased slightly during bathing, it was not significant (**Fig. 6**). Although LF/HF increased slightly during bathing, it was not significant (**Fig. 7**).

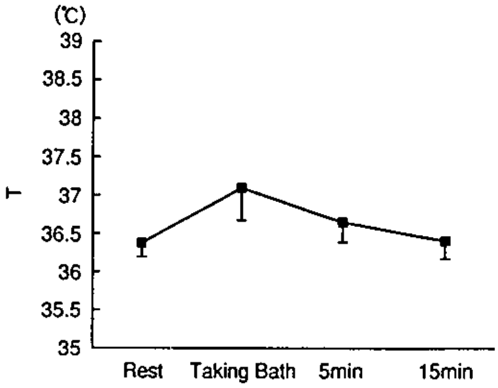

Fig. 1 Rise of the temperature under bathing
By a diagram, it turns out during bathing that temperature is rising.

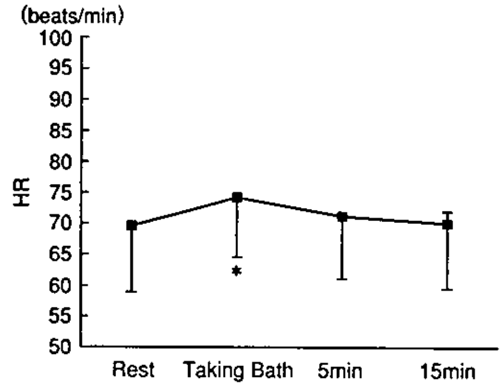

Fig. 2 Heart rate under bathing
The heart rate increased significantly during bathing, while blood pressure decreased significantly.

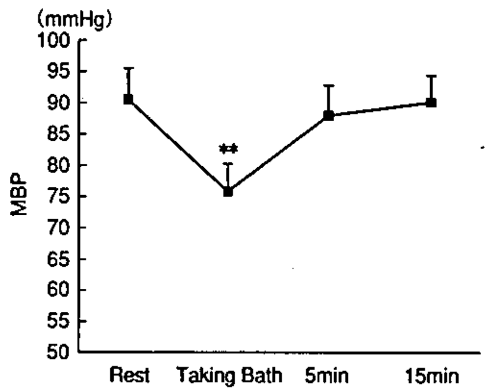

Fig. 3 Mean blood pressure (MBP) under bathing
The MBP decreased significantly during bathing, while blood pressure decreased significantly.

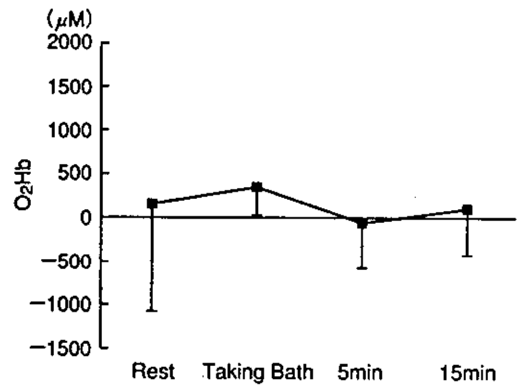

Fig. 4 Brain tissue oxygen metabolism of the frontal lobe
Although O_2Hb was not significant, it showed an upward trend.

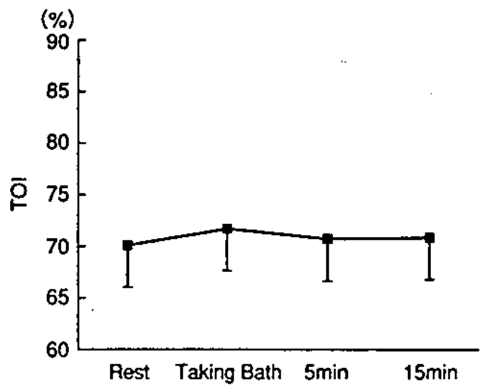

Fig. 5 Tissue oxygen index (TOI) in the brain tissue of the frontal lobe
Although TOI was not so significant altered.

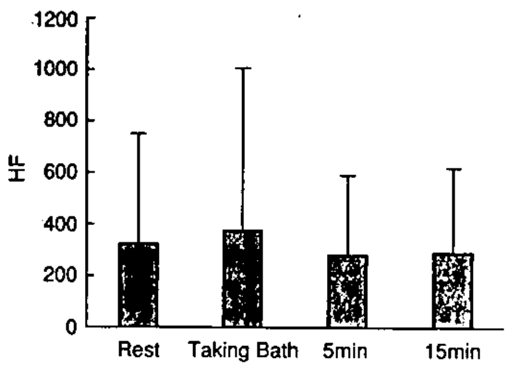

Fig. 6 HF in the spectrum analysis result of a heart rate variability

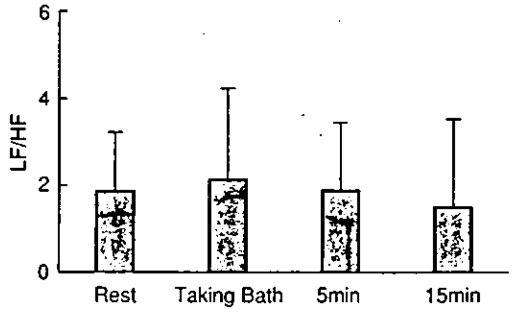

Fig. 7 LF/HF in the spectrum analysis result of a heart rate variability

Discussion

There are many patients who call an ambulance due to apoplexy during bathing. There are few reports of the brain blood flow under bathing. Invention of a NIRO monitoring device enabled this approach.

Our research found that blood pressure falls during bathing and the heart rate increases. This is considered due to the peripheral blood vessel being opened by bathing. If a peripheral blood vessel opens, blood vessel resistance will fall. To maintain blood pressure, the heart rate goes up. If the heart rate goes up, cardiac output increases. If cardiac output increases, blood pressure returns.

Autonomic nerves play an active part in this process. HF and LF/HF increased slightly. This data supports this reaction. As for not being significant, N was considered because it is limited. From now on, it is necessary to increase N.

The result of the cerebral oxygen metabolism in tissue is important. O_2Hb and TOI increased slightly during bathing. This result suggests an increase in brain blood flow. Intellectual activity was not carried out during bathing. Therefore, it is considered that oxygen consumption of brain tissue is fixed. It is considered that O_2Hb increased because supply increased. The result of TOI also supported this consideration. The increase in brain blood flow may be desirable. However, a person with frail blood vessels is at risk. Intracerebral bleeding during bathing may originate in the increase in blood flow. The fall of blood pressure may be desirable. However, it is dangerous in certain illnesses. If blood pressure falls, brain blood flow will fall in those who have arteriosclerosis in a brain artery. The fall of a brain blood flow relates to cerebral infarction. This reduction may relate to the cerebral infarction during bathing. A desirable action may also be dangerous for a sick person.

Sick people need to be cautious when bathing.

Acknowledgements

This paper was presented in part at 8th Congress of the Nonlinear Cardiology held at Tokyo, JAPAN. The authors thank Mr. Kimio Kikuchi for experimental preparation and kind cooperation, Miss Yoko Ito, and Mrs. Hisako Iijima for their excellent technical assistance and kind cooperation.

This work was partly supported by a Grant-in-aid for Scientific Research (11480253), Research Grant for Cardiovascular Diseases from the Ministry of Health and Welfare and Program for Promotion of Fundamental Studies in Health Science of Organizing for Drug ADR Relief, R & D Promotion and Product Review of Japan.

References

1) Boone T, Westendorf T, Ayres P. Cardiovascular responses to a hot tub bath. J Altern Complement Med 1999;5(3):301-4.
2) Rissmann A, Al-Karawi J, Jorch G. Infant's physiological response to short heat stress during sauna bath. Klin Padiatr 2002;214(3):132-5. PMID：12015647 [PubMed-indexed for MEDLINE]
3) Gribanov AN, Dvornikov VE. Spectral analysis of the variability of heart rhythm in the analysis of changes in the autonomic regulation during treatment of hypertension with sodium chloride baths. Vopr Kurortol Fizioter Lech Fiz Kult 2001;(6):13-6.
4) Hentschel HD, Blanco BR, Iser H. On the problem of ECG changes during the taking of arm baths with rising temperature. Arch Phys Ther (Leipz) 1965;17(4):287-92.
5) Yorifuji S, Takahashi M, Ogasahara S, Nakamura Y, Hazama T, Mitomo M, Tarui S. Focal luxury perfusion with an early-filling vein in relation to neurological symptoms evoked by heat. J Neurol 1985;232(1):58-9.
6) Gilzean N. Taking to the waters. Nurs Mirror 1984;158(5):34-5.
7) Andreev SV, Tarasenko AT. Effect of the water temperature on body irradiation in taking radon baths. Vopr Kurortol Fizioter Lech Fiz Kult 1981;(1):12-4.
8) Koivisto VA. Sauna-induced acceleration in insulin absorption from subcutaneous injection site. Br Med J 1980;280(6229):1411-3. PMID：7000239 [PubMed-indexed for MEDLINE]
9) Henderson RG. Bath-taking made easy. Br Med J 1976;2(6042):1008.
10) Yambe T, Yoshizawa M, Taira R, Tanaka A, Tabayashi K, Sasada H, Nitta S. Chaos attractors of ventricular elastance to evaluate cardiac performance. Artif Organs 2003;27(1):104-7.
11) Yambe T, Yoshizawa M, Taira R, Tanaka A, Iguchi A, Tabayashi K, Tobita S, Nitta S. Fluctuations of Emax of the left ventricle：effect of atrial natriuretic polypeptide. Biomed Pharmacother 2001;55 Suppl 1:147s-52s.
12) Yambe T, Nanka S, Kobayashi S, Tanaka A, Owada N, Yoshizawa M, Abe K, Tabayashi K, Takeda H, Nishihira T, Nitta S. Detection of the cardiac function by fractal dimension analysis. Artif Organs 1999;23(8):751-6.
13) Yambe T, Nanka S, Kobayashi S, Tanaka A, Yoshizawa M, Abe K, Tabayashi K, Takeda H, Nitta S. Origin of chaos in the circulation：open loop analysis with an artificial heart. ASAIO J 1998;44(5):M700-3.
14) Yambe T, Abe Y, Yoshizawa M, Imachi K, Tabayashi K, Takayasu H, Takeda H, Gouhara K, Nitta S. Strange hemodynamic attractor parameter with 1/R total artificial heart automatic control algorithm. Int J Artif Organs 1996;19(5):302-6.

Artificial Baroreflex System Makes Deterministic Chaos

Tomoyuki YAMBE, Mune-ichi SHIBATA, Makoto YOSHIZAWA,
Yusuke ABE, Kou IMACHI, Akira TANAKA,
Ken-ichi ABE, Hidetoshi MATSUKI, Shigenao MARUYAMA,
Toshiyuki TAKAGI, Yun LUO, Tasuku YAMAGUCHI
and Shinichi NITTA

日本臨床生理学会雑誌　第 33 巻 第 3 号　別刷

平成 15 年 6 月 1 日 発行

INTRODUCTION

Biomedical-engineering research was chosen as the 21st century COE by governmental selection in Tohoku University. This COE team is due to develop various Biomedical-Engineering researches. In Tohoku University, research and development of an artificial organ have been done from dozens of years before.[1-5] The first clinical success case in Japan of a ventricular assist device was acquired in Tohoku University Hospital. The medical treatment examination headquarters of the ventricular assist device of Nippon Zeon was assigned in Tohoku University (Fig. 1).

Recently, various artificial organs are developed.[6-10] The 21st century COE program of Tohoku University thinks artificial organ development as important. Artificial organ development especially using nanotechnology is performed.

In Tohoku University, the sensor for living bodies with the structure of nano level is developed. Since this sensor is excellent in durability, it is the best for an artificial organ. We have succeeded also in development of the control chip computer of micro level. In the combination of a nano sensor and a microchip computer, a nano baroreflex system takes shape.

The cell structure of a living body is micron level. If it succeeds in the baroreflex system development of nano level structure, the cell structure of a living body will be exceeded.

The 21st century COE program promotes the nano biotechnology research which exceeds the function of a living body. Therefore, development of a nano artificial baroreflex system is tried in this study.

VARIOUS ARTIFICIAL HEART AND VARIOUS AUTOMATIC CONTROL ALGORITHM

In a hospital, various artificial organs are used for the various purpose.[1-10] Various artificial circulation equipments are developed. It is roughly divided into a total artificial heart and a ventricular assist device. A total artificial heart replaces the natural heart after surgical removal (Fig. 2). Therefore, a total artificial heart is asked for a perfect performance.

On the other hand, a ventricular assist device is equipment with which circulation is assisted. Various circulation assist devices have been developed until now.

The system which can be used easily is desirable in the emergency spot. Percutaneous cardiopulmonary support system (PCPS) is easy and useful. Circulation is maintainable from an emergency unit to an operating room. However, PCPS cannot be used for a long time. A thrombus tends to adhere to artificial lungs and a rotary pump. Prolonged use of PCPS is dangerous. There are many patients whom circulation does not recover in a short time. The assist device which can be used more for a long time is required for such a

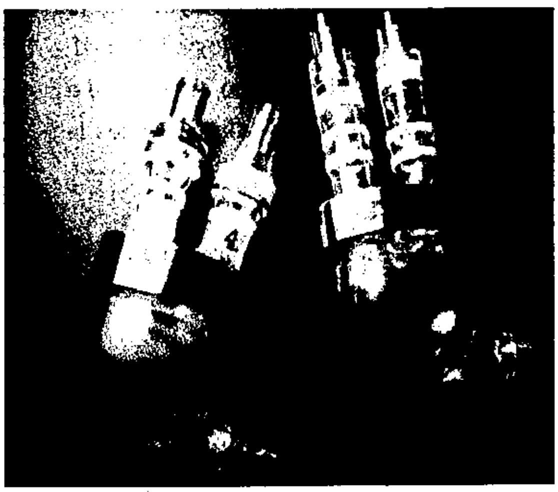

Fig. 1 Nippon Zeon ventricular assist device developed in Tohoku University.

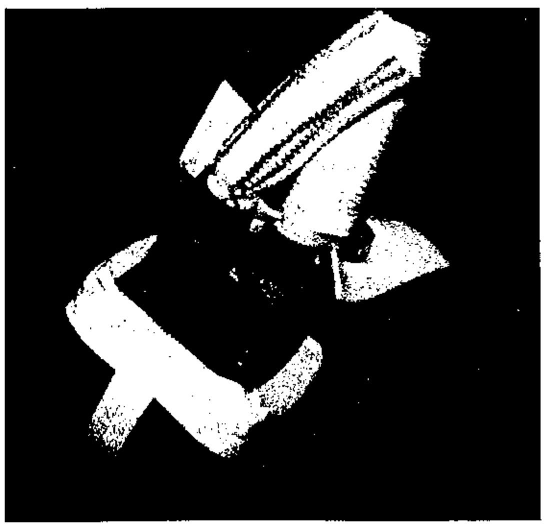

Fig. 2 Pneumatic driven total artificial heart developed in Tohoku University.

patient.

In Japan, the ventricular assist device of an air pressure drive is used for such the patient (Fig. 1). When using air pressure drive type equipment, it is not separated from a driving gear by the patient. Substantially, a patient becomes bedridden in ICU.

For the quality of life (QOL), a complete-implantable type is desirable. Now, many implantable type ventricular assist devices are developed overseas. However, the artificial heart developed in Europe and America is too large.

Small VAD is desired for Japanese people.

In order to miniaturize, there is also a method using rotary blood pump (RP).[11,12] However, a pulse is lost in RP. Then, we made frequency increase. If frequency is made to increase, the chamber will be made small. Then, a small artificial heart can be made. And it is also a capacity type blood pump. Therefore, a pulse can be made easily. This is the major candidate of a small artificial heart.

The new methodology to which frequency is made to increase using rotation had developed. It is the new artificial heart called undulation pump artificial heart (UPAH). Undulation movement is changed into pump movement in this artificial heart (Fig. 3). Now, a total artificial heart is manufactured and it is used for the animal experiment.

Moreover, we had made the artificial myocadium.

In this system, a machine pushes the heart. It is the same as the heart massage in the emergency spot. Therefore, the validity of a principle is established. We used the ball screw type electromagnetic motor (Fig. 4). It is the same principle as the robot arm of a space shuttle. Therefore, it excels in durability. Small auxiliary circulation is attained by this.

Thus, there are various artificial hearts. Various artificial hearts are used for the various purpose. There are the various controlling methods in various artificial hearts. However, it is the same at the point of maintaining circulation. Then, a common control algorithm is needed. We invented the control system common to all artificial circulation equipments.

ARTIFICAL BAROREFLEX SYSTEM

A control system is important for maintenance of homeostasis. The baroreflex system is one of the typical things of homeostasis. In human's body, if blood pressure goes up, a heart rate will fall. Since a heart rate falls, a cardiac output falls. Blood pressure will become low if a cardiac output decreases. Therefore, blood pressure is maintained by the fixed range. This is the main action of a baroreflex system.

However, there is no baroreflex system in an artificial heart.[13-16] Even if blood pressure goes up, a heart rate does not change. Therefore, hypertension is maintained. With the artificial heart research institution in the world, high blood pressure has occurred to the animal with an artificial heart. Therefore, it is thought

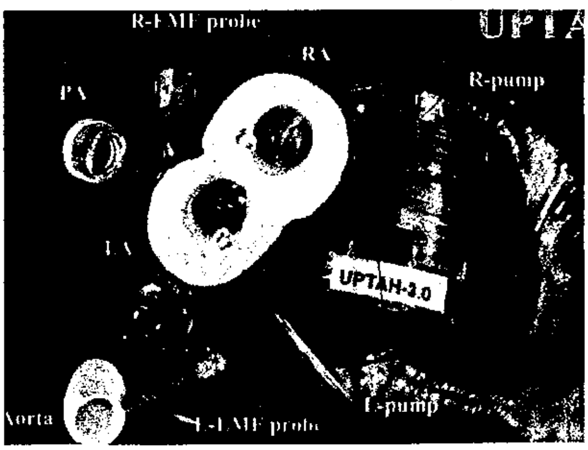

Fig. 3 Totally implantable undulation type artificial heart system.

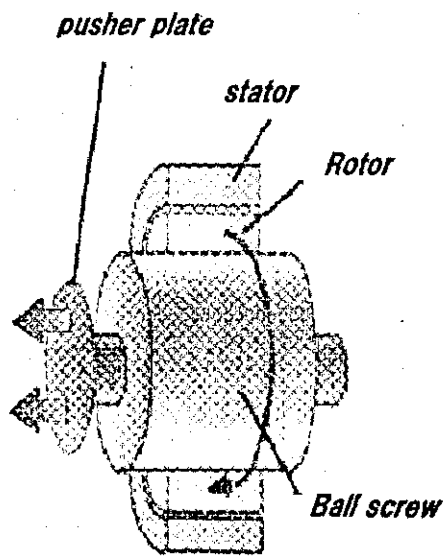

Fig. 4 Electromagnetic motor of a ball screw type for an implantable artificial myocardium.

that a baroreflex is required for an artificial heart.

We developed the control system which imitated the baroreflex for the artificial heart. The animal experiment was conducted with the mathematics simulation and the hydraulics simulation. Consequently, the validity of baroreflex control was proved.

MATHEMATICAL SIMULATION OF AN ARTIFICAL BAROREFLEX SYSTEM

First, the mathematical model was created.

Windkessel model was used for the model of left-heart circulation. This is the typical model which many researchers have used.[17-19] We added the baroreflex system to this famous model (Fig. 5). If blood pressure goes up, control to which a cardiac output decreases will be added. Human's body holds nonlinearity. Then, nonlinearity was introduced into this relationship. For that purpose, a sigmoid curve is used. Furthermore, as for an important thing, there is time lag in human's control system. Even if disturbance is added, it will take time, before a reaction from the control system comes out. Therefore, time lag is required for the simulation of a control system.

The simulation showed the interesting result. A result changes with values of time lag. If time lag is short, blood pressure will be converged on a fixed value. It was the result of showing classic homeostasis.

However, if time lag is long, blood pressure will not become a fixed value but will be oscillated. Furthermore, blood pressure became chaos when time lag was long.

This was a surprising result. Time lag had played the role important for generating of chaos.

We confirmed this result by other experiment systems.

ANIMAL EXPERIMENT SHOW THE UNIVERSALITY OF THE ARTIFICIAL BAROREFLEX SYSTEM

It was applicable to all artificial hearts. It was applicable to RP and PCPS. The baroreflex which reacts even if there is no pulse was a surprising research result. Human's baroreflex is because it happens for a pulse.

A receptor for a baroreflex system in human body generates a signal in the portion of the standup of a pulse. Many researchers have reported this phenomenon. Therefore, baroreflex control of a living thing cannot be performed without a pulse. RBAC control does not necessarily need a pulse, if information is inputted. It is the automatic control system which exceeds a life phenomenon in a sense.

Is such a thing truly possible?

We showed the result. The experiment was conducted by the animal experiment of full bypass circulation with RP. The heart was electrically fibrillated, and all

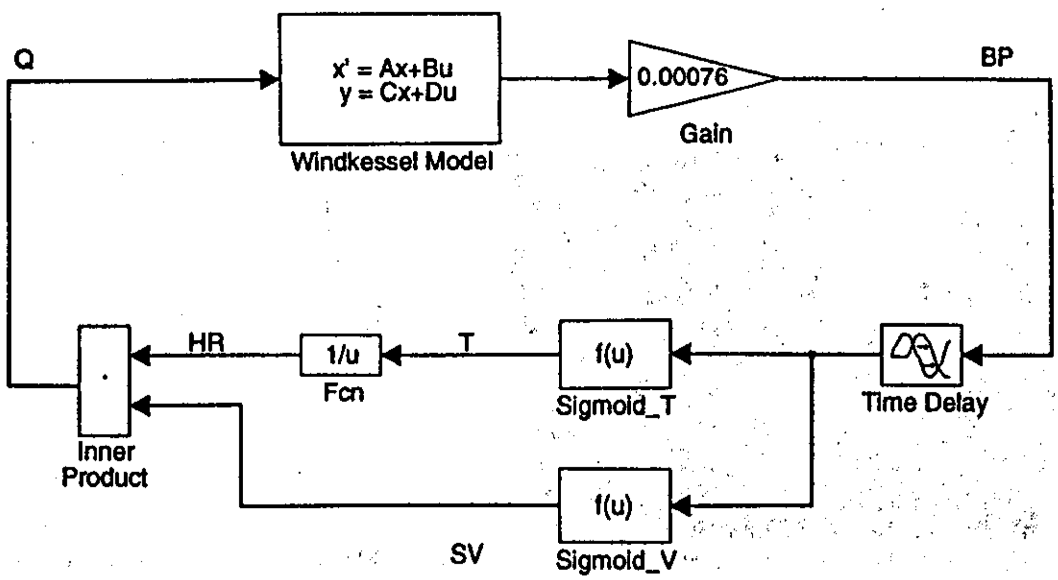

Fig. 5 Block diagram of the mathematical model of a baroreflex system.

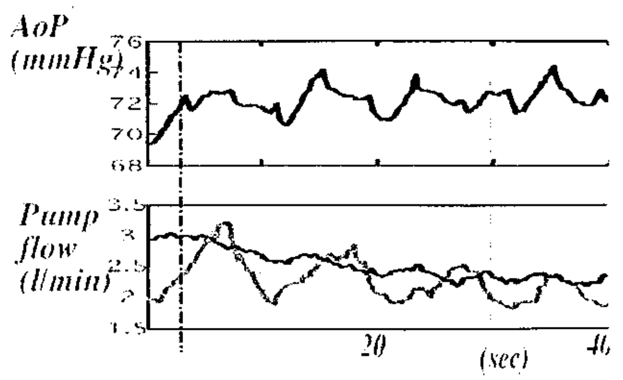

Fig. 6 Time series data of the total nonpulsatile circulation with a baroreflex system during drug administration.

circulation was maintained only by RP. Therefore, there was no pulse.

However, baroreflex control was possible as shown in Fig. 6. Fluctuation of a hemodynamics was observed in the figure. When blood pressure was changed with the medicine, the automatic control system reacted. Blood pressure returned by the automatic control system.

As a result, circulation without a pulse was also possible for the baroreflex by our RBAC system.

It is also an interesting result that fluctuation occurred although there is no pulse. The circulation in which human beings do not have a pulse has not been experienced. Therefore, it is not known whether there is any fluctuation by the artificial heart without a pulse. Now, RP is used as an assisted circulation by clinical. However, a total artificial heart is not made into non-pulsation by clinical. There was little research done non-pulsation by the total artificial heart.

Fluctuation was discovered by perfect non-pulsation circulation by this research. This fluctuation is the very interesting result of being in agreement also with a mathematical model.

These results may be able to be called surprising.

The baroreflex impossible for all lives without a pulse became possible. The life which had a baroreflex system without a pulse for the first time on the earth was born.

Furthermore, it was the result of bringing a new view to the possibilities of RP. For the miniaturization of an artificial heart, RP is absolutely advantageous. Since a pumping chamber is not needed, it is only a rotary motor. The problem was that there is no pulse. If there is no pulse, autonomic control in a life will not be performed. Also physiologically, it was a problem.

RBAC control may be able to solve this problem. When human's body needs, a circulatory state must change. Our control can respond to this change. Therefore, the life excellent in QOL is attained. Because we can catch up the need of your body.

The application to a present still newer artificial circulation system is under plan. It is the artificial myocardium plan which received the research cost of 120 million from the Ministry of Health, Labor and Welfare. The present implantable type artificial myocardium plan is progressing in Tohoku University, making full use of the latest nanotechnology.

Into artificial myocardium, it is due to be equipped with the baroreflex control with a nano sensor and a nano computer chip. Arrival of the society which does not die of cardiovascular diseases is desired by the newest artificial myocardium.

This paper was presented in part at 6th Congress of Clinical Application of Chaos Analyzing Methodology Meeting in Kanazawa, Japan. The authors thank Mr. Kimio Kikuchi for experimental preparation and kind cooperation, Miss Yoko Ito, and Mrs. Hisako Iijima for their excellent technical assistance and kind cooperation.

This work was partly supported by a Grant-in-Aid for Scientific Research (11480253), Research Grant for Cardiovascular Diseases from the Ministry of Health and Welfare and Program for Promotion of Fundamental Studies in Health Science of Organizing for Drug ADR Relief, R&D Promotion and Product Review of Japan.

REFERENCES

1) Yambe T, Kawano S, Nanka S, Kobayashi S, Tanaka A, Owada N, Yoshizawa M, Abe K, Tabayashi K, Takeda H, Hashimoto H, Nitta S: Peripheral vascular resistances during total left heart bypass with an oscillated blood flow. *Artif Organs* 1999, **23**(8): 747–750
2) Yambe T, Owada N, Kobayashi S, Sonobe T, Naganu-

ma S, Nanka S, Hashimoto H, Yoshizawa M, Tabayashi K, Takayasu H, Takeda H, Nitta S: Left heart bypass using the oscillated blood flow with totally implantable vibrating flow pump. *Artif Organs* 1998, **22**: 426–429

3) Yambe T, Nitta S, Sonobe T, Naganuma S, Kakinuma Y, Kobayashi S, Nanka S, Ohsawa N, Akiho H, Tanaka M, et al.: Origin of the rhythmical fluctuations in the animal without a natural heartbeat. *Artif Organs* 1993, **17**(12): 1017–1021

4) Yambe T, Nitta S, Katahira Y, Sonobe T, Naganuma S, Kakinuma Y, Akiho H, Izutsu K, Kikuchi Y, Tanaka M, et al.: Dependence of baroreceptor mediated sympathetic outflow on biventricular assist device driving frequency. *Artif Organs* 1993, **17**(1): 18–23

5) Yambe T, Nitta S, Katahira Y, Sonobe T, Tanaka M, Miura M, Satoh N, Mohri H, Yoshizawa M, Takeda H. Effect of left ventricular assistance on sympathetic tone. *Int J Artif Organs* 1990, **13**(10): 681–686

6) Kimoto S, Atsumi K, Sakurai Y, Yamazaki Z, Isayama T, Fujimori Y, Uchida R: Studies on the artificial heart driven with controlled gas pressure device on the pressure generator for universal use. *Trans Am Soc Artif Intern Organs* 1964, **10**: 66–68

7) Freebairn D, Heggs T: Solenoid design for a prosthetic heart. *Trans Am Soc Artif Intern Organs* 1964, **10**: 166–171

8) Akutsu T, Topaz SR, Mirkovitch V, Panayotopoulos E, Kolff WJ: Problems in calf lungs immediately after implantation of an artificial heart. *Trans Am Soc Artif Intern Organs* 1964, **10**: 162–165

9) White RJ: Related Articles, Links Artificial heart: a medical miracle. *Artif Organs* 2002, **26**(12): 1007–1008

10) Weber S, Doi K, Massiello AL, Byerman BP, Takagaki M, Fukamachi K, Donahue A, Chapman P, Hirschman G, Vitale N, Smith WA: In vitro controllability of the MagScrew total artificial heart system. *ASAIO J* 2002, **48**(6): 606–611

11) Nojiri C, Kijima T, Maekawa J, Horiuchi K, Kido T, Sugiyama T, Mori T, Sugiura N, Asada T, Shimane H, Mishimura K, Ban T, Akamatsu T, Ozaki T, Ito H, Suzuki M, Akutsu T: More than 1 year continuous operation of a centrifugal pump with a magnetically suspended impeller. *ASAIO J* 1997, **43**: M548–552

12) Greiner AS, Skeehan TM, Larach DR, Schuler HG, Pierce WS: Vascular responses to dopamine and dobutamine in the awake calf during constant aortic flow or constant aortic pressure. *J Cardiovasc Pharmacol* 1990, **15**(3): 392–397

13) Smyth HS, Sleight P, Pickering GW: Reflex regulation of arterial pressure during sleep in man. A quantitative method of assessing baroreflex sensitivity. *Circ Res* 1969, **24**(1): 109–121

14) Bristow JD, Honour AJ, Pickering GW, Sleight P, Smyth HS: Diminished baroreflex sensitivity in high blood pressure. *Circulation* 1969, **39**(1): 48–54

15) Mallie JP, Osman H, Danjou MA, Coquelet O, Helot MF, Flandrois R: Experimental study of the baroreflex ventilatory stimulus. *J Physiol (Paris)* 1968, **60**(2): 491

16) Alexander N, DeCuir M: Sinoaortic baroreflex system and early pressure rise in renal hypertensive rabbits. *Am J Physiol* 1967, **213**(3): 701–705

17) Cavalcanti S: Arterial baroreflex influence on heart rate variability: a mathematical model-based analysis. *Med Biol Eng Comput* 2000, **38**(2): 189–197

18) Cavalcanti S, Di Marco LY: Numerical simulation of the hemodynamic response to hemodialysis-induced hypovolemia. *Artif Organs* 1999, **23**(12): 1063–1073

19) Cavalcanti S, Belardinelli E: Modeling of cardiovascular variability using a differential delay equation. *IEEE Trans Biomed Eng* 1996, **43**(10): 982–989

ELSEVIER

Available online at www.sciencedirect.com
SCIENCE DIRECT

Sensors and Actuators A 111 (2004) 304–309

SENSORS AND ACTUATORS A PHYSICAL
www.elsevier.com/locate/sna

Three-axis magneto-impedance effect sensor system for detecting position and orientation of catheter tip

Kentaro Totsu [a,*], Yoichi Haga [b], Masayoshi Esashi [c]

[a] Department of Mechatronics and Precision Engineering, Tohoku University, 01 Aza-Aoba, Aramaki, Aoba-ku, Sendai 980-8579, Japan
[b] Department of Bioengineering and Robotics, Tohoku University, 01 Aza-Aoba, Aramaki, Aoba-ku, Sendai 980-8579, Japan
[c] New Industry Creation Hatchery Center (NICHe), Tohoku University, 01 Aza-Aoba, Aramaki, Aoba-ku, Sendai 980-8579, Japan

Received 29 December 2002; received in revised form 18 November 2003; accepted 20 November 2003

Abstract

A catheter-based minimally invasive therapy requires real time information about the position and orientation of a catheter tip for safe operation. To decrease X-ray exposure and to provide 3D information for operators, a simple sensor system for detecting the position and orientation utilizing the earth's magnetic field and ac (10 kHz) magnetic field transmitted by a two-axis source coil is proposed. A 2 mm × 2 mm × 3 mm three-axis MI sensor (Magneto-Impedance effect sensor) fabricated on a polymer structure for measuring the earth's magnetic field and the ac magnetic field is mounted on the catheter tip. The advantages of this sensor are: (1) small size; (2) high sensitivity; (3) retaining of through hole. The position and orientation is calculated and the obtained information of the position and orientation of the catheter tip is superimposed on the 3D map of the blood vessel captured in advance. A measurement in a blood vessel model has been performed and the calculated position and orientation image has been superimposed on the 3D graphic image of the blood vessel. The sensor system obviously indicated where the catheter tip was in the "y" shape blood vessel model.

Keywords: MI sensor; Catheter; Navigation; Position and orientation; 3D

1. Introduction

A catheterization used for the minimally invasive therapy has been widely carried out. Doctors can access to diseased area via blood vessel by insertion of a catheter and can do therapy with minimally invasion. In the therapy using the catheterization, real time information about the position and orientation of a catheter tip is necessary for safe navigation in the blood vessel. Generally, X-ray radioscopy is used to monitor the position and orientation of a catheter. However X-ray radioscopy can provide only two-dimensional (2D) images and requires an X-ray shielded room. Besides doctors must put on a heavy protector during the procedure and a long time X-ray exposure is harmful to patients and medical staff. As blood vessel is distributed three-dimensionally, it is helpful for navigation of a catheter if 3D image can be obtained. And navigation system without X-ray exposure is preferable for patients and doctors. In order to detect a three-dimensional (3D) position and orientation of an object, magnetic, optic, ultrasonic and mechanical sensors are mostly employed. A lot of magnetic detecting systems have already developed and commercialized [1–9]. The magnetic detection systems have some advantages.

1. Disturbance of magnetic field in a human body can be ignored because the permeability of human body is nearly equal to 1, which is equal to the permeability of the air.
2. A magnetic field is regarded safe if appropriate frequency and intensity are used.
3. A miniaturization of a magnetic sensor is relatively easy.

A magnetic position and orientation detecting system has been commercialized for monitoring the shape of an endoscope [7]. The coils are built in the endoscope and transmit magnetic fields. The outer diameter of the endoscope is about 12 mm. The other application is electrophysiological mapping and positioning of the site for RF catheter ablation in a heart [8,9]. The coils are built in the catheter tip and detect magnetic fields transmitted by external source coils. However the outer diameter of the tip is relatively small (3 mm), there is no through hole for inserting micro tools (e.g., guide wire) and injection of contrast medium and drug. In this paper, a simple real time catheter navigation system using a small three-axis magneto-impedance effect sensor, with less

* Corresponding author. Tel.: +81-222176937; fax: +81-222176935.
E-mail address: totsu@mems.mech.tohoku.ac.jp (K. Totsu).

0924-4247/$ – see front matter © 2003 Elsevier B.V. All rights reserved.
doi:10.1016/j.sna.2003.11.018

X-ray exposure during a catheterization is proposed. The sensor system can be applied to not only a catheter but also other small tools for minimally invasive therapy, such as an endoscopic procedure.

2. System concept

Fig. 1 shows the proposed catheter navigation sensor system. Before a catheterization, 3D image data of the blood vessel of a patient is captured by X-ray CT or MRI and is stored in a computer. During the catheterization, the position and orientation of the tip of the catheter is detected by a magnetic sensor built in the tip of the catheter. A cursor which indicates the position and orientation of the catheter is superimposed on the 3D internal image of the human body (e.g., blood vessel). This system can be useful for 3D navigation in other organs and tracts, e.g. branches of bronchus, digestive systems (stomach, duodenum, colon) and urinary tract for more precise operation in the human body.

If this sensor system is compared to a commercialized car navigation system, a catheter tip corresponds to a car and blood vessels correspond to roads. An operator can control the catheter tip in blood vessel as if the operator drives a car on the road.

As shown in Fig. 1, the sensor composed of three orthogonal magnetic sensor elements detects the earth's magnetic field as a dc field and ac (10 kHz) magnetic fields transmitted by a two-axis source coil placed near the patient. A 3D orientation of the sensor is represented by three Euler's angles [10]. A measurement of the earth's magnetic field is used to obtain two of Euler's angles, measurements of two ac magnetic fields are used to obtain the remaining one of Euler's angles and a 3D position of the sensor [11].

3. Sensor

3.1. Principle of sensor

Concerning the sensor characteristics, the three-axis magnetic sensor detects the earth's magnetic field and the ac magnetic field simultaneously to achieve the algorithm, and the size of the sensor should be less than 2 mm in order to built in a catheter. In several magnetic sensors, Magneto-Impedance effect sensor (MI sensor) has received attention recently because of its high sensitivity (10^{-10} T), high response speed (MHz), low power consumption (10 mW using CMOS IC) and small size (1∼2 mm) [12,13]. Therefore the MI sensor was selected for our sensor system. The MI sensor utilizes an electromagnetic phenomenon in which an impedance Z of electrically conductive magnetic materials magnetized with a high frequency current inducing the skin effect is sensitively changed with an applied external magnetic field (MI effect) [12]. As the sensor head, an amorphous wire type is often used because of its high sensitivity compared to a thin film type. The impedance Z of a wire of the MI sensor head is expressed as [12]

$$|Z| \approx \frac{a}{2\sqrt{\rho}} R\sqrt{\omega\mu_\theta}$$

where a is a radius, l a length, ρ a resistivity, μ_θ a circumferential permeability magnetized with a sinusoidal current with angular frequency ω and $R = \rho l/\pi a^2$ is the dc resistance.

If the impedance $|Z|$ is measured, intensity of the external magnetic field can be detected because the μ_θ is sensitively changed by the external magnetic field parallel to the MI sensor.

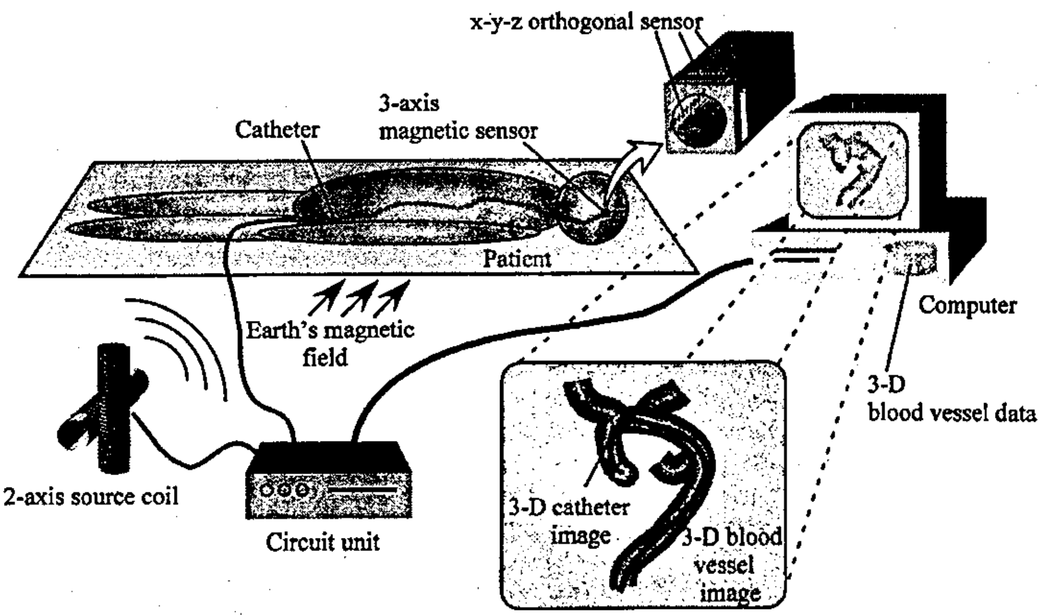

Fig. 1. Schematic of sensor system.

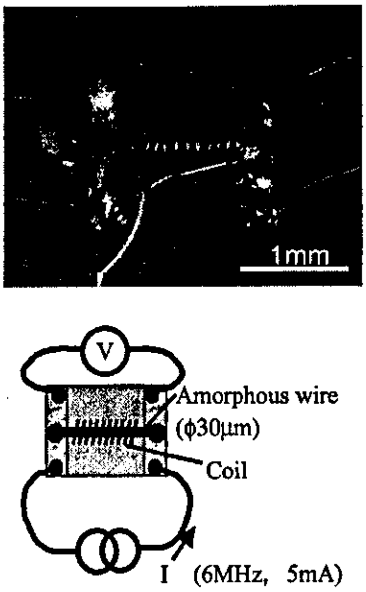

Fig. 2. Structure of MI sensor.

3.2. Fabrication of sensor

A MI sensor as a test type was fabricated as shown in Fig. 2. A FeCoSiB amorphous wire of 30 μm in diameter and of 1.5 mm in length was fixed at the center of a glass epoxy substrate and electrically connected to electrodes by using conductive epoxy. The four lead wires were also connected to the electrodes by soldering to pass current (6 MHz, 5 mA) and to detect voltage between the both sides of the amorphous wire to measure impedance of the wire. In order to apply a bias magnetic field, the amorphous wire is surrounded by a small coil. To transfer the signals, ultra-small diameter coaxial cables (Sumitomo Electric Industries 44110T) of 250 μm in outer diameter, and of 1 m in length were used between the sensor and the circuit. A 6 MHz sinusoidal voltage modulated at 10 kHz equal to the frequency of the transmitted ac magnetic field was obtained and processed at the circuit. The characteristics of the sensor using a differential amplifier is shown in Fig. 3. The impedance curve has assumed a minimum at 0 T without bias coil current. As the bias coil current shifts the impedance curve, polarity of the external dc magnetic field can be determined.

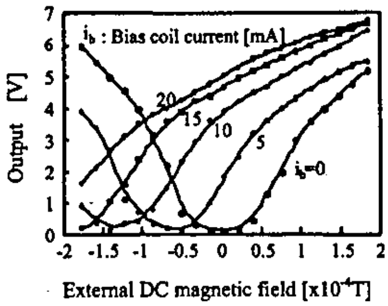

Fig. 3. Characteristics of MI sensor with changing of bias coil current.

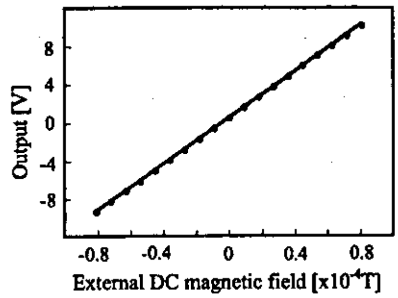

Fig. 4. Characteristics of MI sensor for external dc magnetic field.

In the circuit, the signal processing was carried out as follows: (1) differential amplification; (2) detection by using a diode; (3) smoothing by using capacitors; (4) separation of AC(10 kHz) component and DC(earth's magnetic field) component; (5) negative feedback of a output of the dc component to the passing current of the bias coil to improve linearity.

In order to determine a direction of the sensor, phase of the ac magnetic field was detected. Therefore 10 kHz current synchronized to the ac magnetic field passed the bias coil as AC bias current. If the detected signal and the bias current are in phase, the output of the circuit is positive. If they are out of phase, the output of the circuit is negative. The result of a measurement of dc magnetic field and ac magnetic field are shown in Figs. 4 and 5 respectively. High sensitivity and high linearity have been achieved.

A three-axis MI sensor was fabricated by integration of three MI sensors on a polymer structure by using epoxy glue as shown in Fig. 6a And the sensor was covered with silicone rubber tube as shown in Fig. 6b. Precise orthogonal alignment of the three MI sensors was required to decrease interference between three-axis components. A polymer structure which had three grooves and patterned electrodes was used to eliminate alignment error of the three orthogonal sensors and to make fabrication easy. The size of the polymer structure was 2 mm × 2 mm × 3 mm. A through hole at the center of the structure is used for inserting micro tools (e.g., guide wire) or injection contrast medium and drug. The structure was fabricated by machining and the electrodes were formed by electro-less plating. In the future, a cheaper polymer

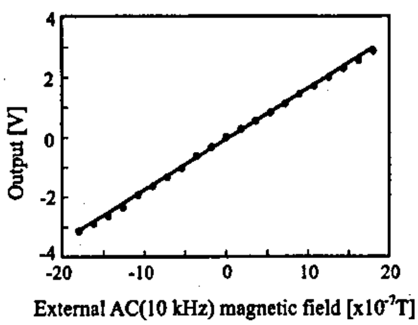

Fig. 5. Characteristics of MI sensor for external ac (10 kHz) magnetic field.

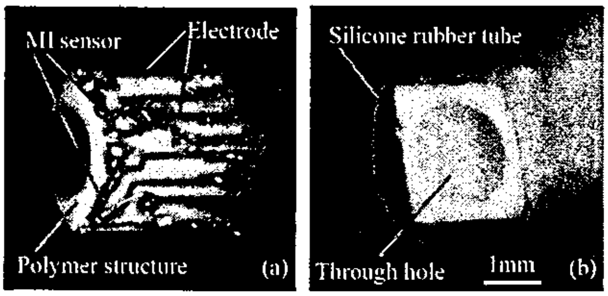

Fig. 6. Fabricated three-axis MI sensor on polymer structure: (a) and covered with silicone rubber tube (b).

structure can be obtained as the base structure of the sensor by using injection molding. A smaller size three-axis MI sensor without a through hole has been also fabricated as shown in Fig. 7. The size of the sensor is 1 mm × 1 mm × 1 mm. These small three-axis MI sensors can be placed in small medical tools (e.g., a guide wire and the tip of the forceps).

3.3. Sensor system

The sensor system is shown in Fig. 8. The output signal transferred from the three-axis MI sensor was processed at the circuit and acquired by a computer via an analog-digital converter. A function generator sent dc biased 10 kHz signal to the circuits for sensing and also sent 10 kHz signal to the source coils via a MOS switch and amplifiers. The MOS switch was controlled by digital signal transmitted from the computer via a digital output port. A two-axis solenoid was fabricated as the source coil. The length and diameter of each axis coil were 10 mm and 40 mm respectively. The coil was composed of a ferrite core and insulated cupper wire. A capacitor was put in parallel to make a resonant circuit at 10 kHz. An application program was built for control the sensor system, calculation based on the algorithm and indication the position and orientation.

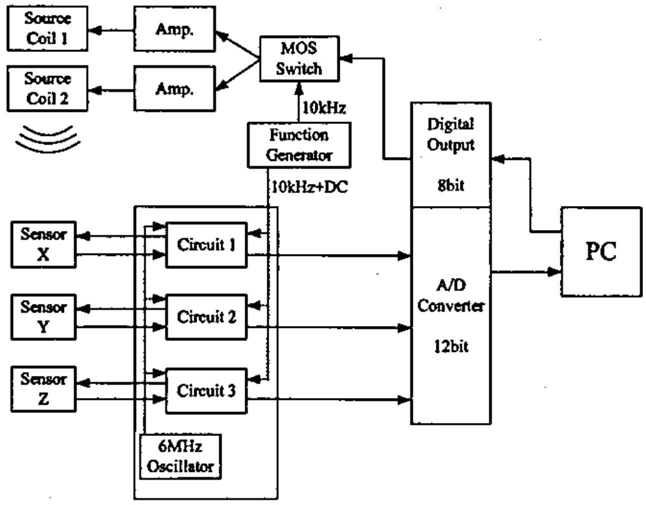

Fig. 8. Configuration of sensor system.

4. Experimental results

The resolution and the error of 3D position and orientation of the developed sensor system were measured. For a position measurement, the three-axis MI sensor was put on a plane parallel to the coordinate of the source coil. The measurement area was 100 mm × 100 mm. The mean of the position error was 2 mm. The maximum 3D position error of 5 mm was occurred and the resolution of the 3D position was about 0.4 mm around the center area and 1.0 mm around the marginal area respectively. The orientation of the sensor was regarded as a constant when position measurement was performed. An orientation measurement has been also performed. The mean of the rotation angle error of 9° was occurred when the MI sensor was turned 360° on the vertical axis. The resolution was about 1°.

A measurement was performed in a blood vessel model. The model consisted of polymer tubes of which outer

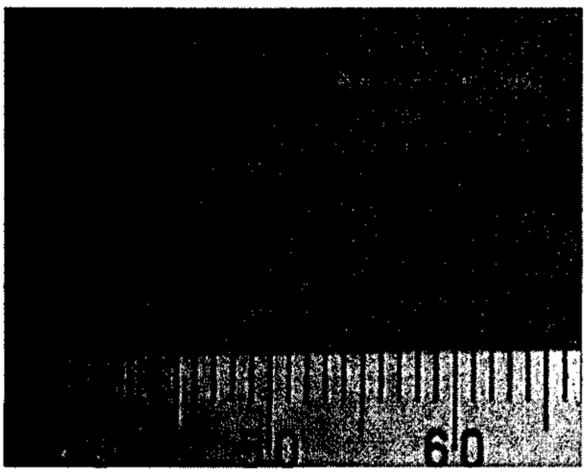

Fig. 7. Fabricated 1 mm size three-axis MI sensor.

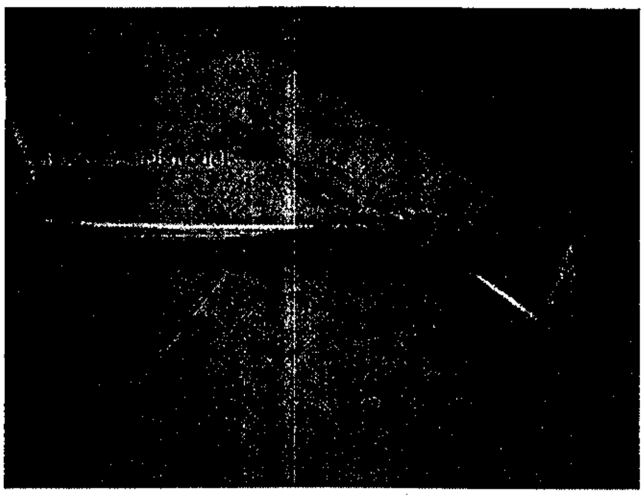

Fig. 9. "y" Branch shape of blood vessel model with inserted three-axis MI sensor.

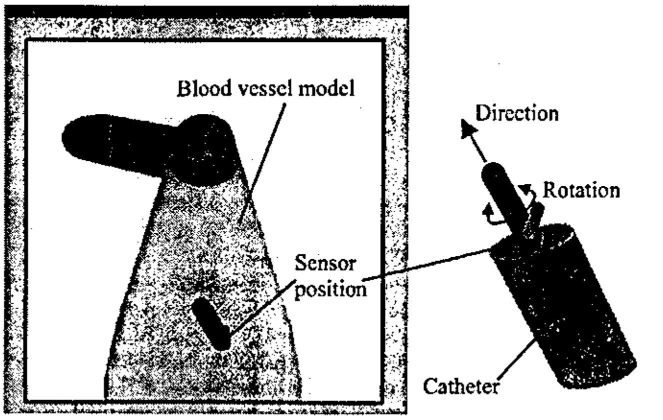

Fig. 10. Sensor position and orientation image superimposed on 3D image of blood vessel model.

diameter and internal diameter are 6 mm and 4 mm respectively as shown in Fig. 9. At the middle point of a tube of 100 mm in length, the other tube was connected for making a "y" branch shape of a blood vessel. The model was placed 100 mm apart from the source coil. A calculated position and orientation image were superimposed on 3D computer graphics of the blood vessel model on a display as shown in Fig. 10. The large bar (black) indicates the direction and the small bar (gray) indicates the rotation around the axis of the catheter respectively. The sensor position can be confirmed on a 2D image as shown in Fig. 11. The sensor was inserted and moved repeatedly in the vessel model and the position and orientation were continuously monitored. The sensor system successfully indicated whether the catheter tip was in the vessel branch or straight part of the vessel on 3D image. A desirable viewpoint and a magnification can be selected using console on the monitor. The mean of axial position error was about 2 mm. The performance of the fabricated smaller three-axis MI sensor (1 mm × 1 mm × 1 mm) was the same for the 2 mm × 2 mm × 3 mm sensor.

5. Discussion

It was considered that the position and the orientation measurement error were mainly caused by distorted distribution of the ac magnetic field transmitted from the source coil, which differ from the ideal distribution. In order to achieve more accurate measurement, the source coil should be precisely designed and fabricated. The measurement area could be extended by using additional source coils. When a magnetic material is placed between the source coil and the sensor, the magnetic field is disturbed and compensation of the magnetic field is difficult. When a non-magnetic metal is placed between the source coil and the sensor, the magnetic field is also disturbed because of eddy current. In this case, the disturbance will be reduced by utilizing pulse magnetic fields instead of the ac magnetic fields. While considering disturbance of the earth's magnetic field in the whole measurement area, it can be compensated if additional sensor is used as a fixed reference sensor to monitor the earth's magnetic field during the measurement. For clinical use, because of movements of a patient after image acquisition, it is necessary to consider difference between the stored image acquired before the operation and the real time image. In this case, additional capturing of 3D image might be required. As our three-axis MI sensor is small and sensitive and also retains through hole, it can be adapted to several medical micro tools, e.g. endoscopes, forceps, RF coagulators and

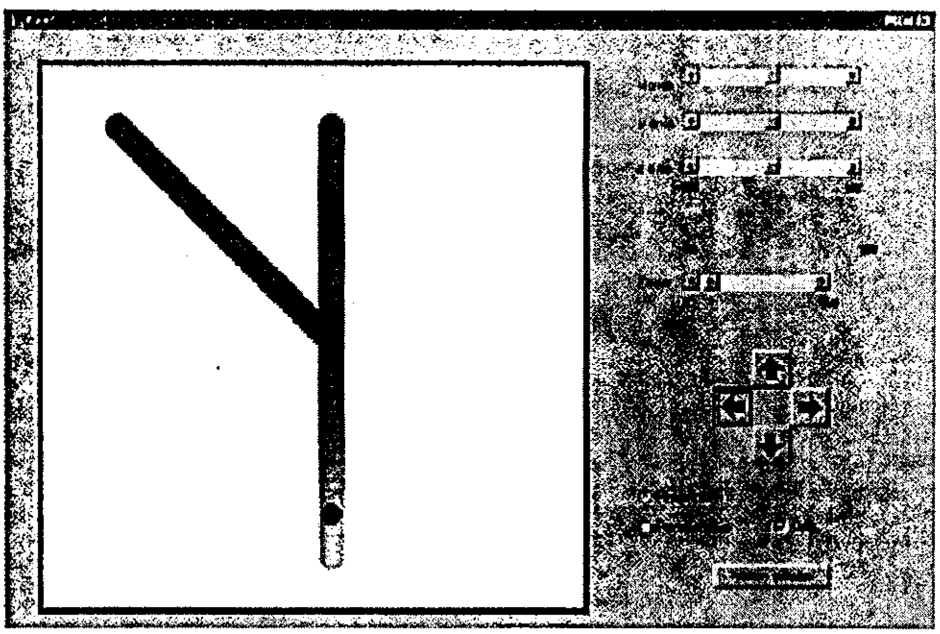

Fig. 11. Sensor position image (black point) superimposed on 2D image of blood vessel model.

laparoscopic micro tools. Another effective medical application of the position and orientation sensor is functional mapping in the human body for example electrophysiological mapping in a heart [8,9].

6. Conclusion

We have developed a three-axis MI sensor system for monitoring the position and orientation of a catheter tip. A novel 3D catheter navigation system using the three-axis MI sensor and 3D internal image of human body has been proposed. The three-axis MI sensor of 2 mm × 2 mm × 3 mm and 1 mm × 1 mm × 1 mm which can be mounted at the tip of the catheter have been developed. The resolution of the position and orientation were 1 mm and 1°, respectively. Detection in blood vessel model has been performed and the position and orientation of the catheter tip is displayed as an indicator on the 3D computer graphics of blood vessel.

Acknowledgements

The authors gratefully acknowledge Prof. K. Mohri (Nagoya University) and Prof. H. Matsuki (Tohoku University) for enligtening advices and discussions. The authors would like to thank Sumitomo Electric Industries, Ltd. and Unitika Ltd. for supplying the ultra-small diameter co-axial cable and the amorphous wire, respectively. This work was supported in part by Micro Machine Center and a Grant-in-Aid (No. 10359001) from the Ministry of Education, Culture, Sports, Science and Technology of Japan.

References

[1] F.H. Raab, E.B. Blood, T.O. Steiner, H.R. Jones, Magnetic position tracker, IEEE Trans. Aerospace Electron. Sys. AES-15 (5) (1979) 709–717.

[2] M. Takayama, K. Maenaka, A. Yamamoto, Position Sensing System Using Integrated Magnetic Sensors And Neural Networks, in: Digest of Technical Papers of Transduccers'01, Munich, Germany, 2001, pp. 76–79.

[3] S. Yabukami, H. Kikuchi, M. Yamaguchi, K.I. Arai, K. Takahashi, A. Itagaki, N. Wako, Motion capture system of magnetic markers using three-axial magnetic field sensor, IEEE Trans. Magn. 38 (2000) 3646–3648.

[4] J.B. Kuipers, SPASYN—an Electromagnetic relative position and orientation tracking system, IEEE Trans. Instrum. Measure. IM-294 (1980) 462–466.

[5] D. Tanase, N.H. Bakker, D.van Loon, J.F.L. Goosen, P.J. Trimp, J.A. Reekers, P.J. French, Radiation dose reduction in minimally-invasive intravascular procedures using a magnetic guidance system, in: Proceedings of Second Annual International IEEE-EMBS Special Topic Conference on Microtechnologies in Medicine & Biology, Madison, Wisconsin, USA, 2002, pp. 305–308.

[6] J.S. Bladen, A.P. Anderson, G.D. Bell, D.J. Heatley, A non-radiological technique for the real time imaging of endoscopes in 3 Dimensions, 1993 IEEE conference record, Nucl. Sci. Symp. Med. Imag. Conf. 3 (1993) 1891–1894.

[7] http://www.olympus.co.jp/LineUp/Endoscope/upd.html.

[8] L. Gepstein, G. Hayam, S.A. Ben-Haim, A novel method for non-fluoroscopic catheter-based electroanatomical mapping of the heart, Circulation 95 (6) (1997) 1611–1622.

[9] S. Shpun, L. Gepstein, G. Hayam, S.A. Ben-Haim, Guidance of radiofrequency endocardial ablation with real-time three-dimensional magnetic navigation system, Circulation 96 (6) (1997) 2016–2021.

[10] R.P. Paul, Robot manipulators: mathematics, programming, and control: the computer control of robot manipulators, MIT Press, Cambridge, USA, 1981.

[11] K. Totsu, Y. Esashi, M. Haga, Magnetic sensor system for detecting position and orientation of a catheter tip, Trans. IEEJ 120-E (5) (2000) 211–218 (in Japanese).

[12] K. Mohri, T. Uchiyama, L.V. Panina, Magneto-Impedance (MI) Micro Magnetic Sensors—Principle and Applications-, in: Digest of Technical Papers of Transduccers'99, Sendai, Japan, 1999, pp. 76–79.

[13] K. Mohri, T. Uchiyama, L.P. Shen, C.M. Cai, L.V. Panina, Sensitive micro magnetic sensor familiy utilizing magneto-impedance (MI) and stress-impedance (SI) effects for intelligent measurements and controls, Sens. Actuators A 91 (2001) 85–90.

Biographies

Kentaro Totsu was born in Kanazawa, Japan, on March 15, 1977. He received his BE and ME degrees in mechanical engineering from Tohoku University in 1999 and 2001, respectively. He is currently pursuing his PhD in mechanical engineering at Tohoku University in which his research concentrates on MEMS-based medical sensors and measurement systems.

Yoichi Haga was born in Sendai, Japan, on April 4, 1965. He received his MD from Tohoku University School of Medicine, in 1992. From 1994 to 1996, he was with Tohoku Kosei-Nenkin Hospital. From 1996 to 2002, he was a research associate in the Department of Mechatronics and Precision Engineering, Tohoku University. He received his PhD degree from Graduate School of Engineering, Tohoku University in 2002. He is currently an assistant professor at the Department of Bioengineering and Robotics, Tohoku University. He has been studying micromachining and nanomachining for medical and welfare application (mainly minimally invasive diagnosis and treatment).

Masayoshi Esashi was born in Sendai, Japan, on January 30, 1949. He received his BE, ME and Doctor of Engineering degrees all in electronic engineering from Tohoku University, in 1971, 1973 and 1976, respectively. From 1976 to 1981, he served as a research associate at the Department of Electronic Engineering, Tohoku University and he was an associate professor from 1981 to 1990. He was a professor at the Department of Mechatronics and Precision Engineering from 1990 to 1998. Since 1998, he has been a professor at the New Industry Creation Hatchery Center (NICHe), Tohoku University. He was the director of the Venture Business Laboratory in Tohoku University from 1995 to 1998. He is also an associate director of the Semiconductor Research Institute. He has been studying micro-sensors and integrated micro-systems. His current research topic is a micro-technology for saving energy and natural resources. He is a member of the IEEE and the IEE of Japan.